Ion microprobe $\delta^{18}O$ analyses to calibrate slow growth rate speleothem records with regional $\delta^{18}O$ records of precipitation

David Domínguez-Villar[a,*], Sonja Lojen[b,c], Kristina Krklec[d], Reinhard Kozdon[e,f], R. Lawrence Edwards[g], Hai Cheng[g,h]

[a] School of Geography, Earth and Environmental Sciences, University of Birmingham, Edgbaston, B15 2TT Birmingham, United Kingdom
[b] Department of Environmental Sciences, Jožef Stefan Institute, Jamova 39, SI-1000, Ljubljana, Slovenia
[c] Faculty of Environmental Sciences, University of Nova Gorica, Vipavska 13, 5000 Nova Gorica, Slovenia
[d] Department of Soil Science, Faculty of Agriculture, University of Zagreb, Svetošimunska 25, 10000 Zagreb, Croatia
[e] Lamont-Doherty Earth Observatory of Columbia University, 10964 Palisades (NY), USA
[f] Department of Geoscience, University of Wisconsin-Madison 1215 West Dayton St. Madison 53706 (WI), USA
[g] Department of Earth Sciences, University of Minnesota, 55455 Minneapolis (MN), USA
[h] Institute of Global Environmental Changes, Xian Jiaotong University, 710049 Xian, China

Abstract

Paleoclimate reconstructions based on speleothems require a robust interpretation of their proxies. Detailed transfer functions of external signals to the speleothem can be obtained using models supported by monitoring data. However, the transferred signal may not be stationary due to complexity of karst processes. Therefore, robust interpretations require the calibration of speleothem records with instrumental time series lasting no less than a decade. We present the calibration of a speleothem $\delta^{18}O$ record from Postojna Cave (Slovenia) with the regional record of $\delta^{18}O$ composition of precipitation during the last decades. Using local meteorological data and a regional $\delta^{18}O$ record of precipitation, we developed a model that reproduces the cave drip water $\delta^{18}O$ signal measured during a 2-year period. The model suggests that the average water mixing and transit time in the studied aquifer is 11 months. On the other hand, we used an ion microprobe to study the $\delta^{18}O$ record of the top 500 μm of a speleothem from the studied cave gallery. According to U-Th dates, this uppermost section of the speleothem was potentially formed during the last decades. The $\delta^{18}O$ record of the top 500 μm of the speleothem has a significant correlation (r^2=0.84; p-value<0.001) with the modelled $\delta^{18}O$ record of cave drip water. Therefore, we confirm that the top 500 μm of the speleothem grew between the years 1984 and 2002 and that the speleothem accurately recorded the variability of the $\delta^{18}O$ values of regional precipitation filtered by the aquifer. We show that the recorded speleothem $\delta^{18}O$ signal is not seasonally biased and that the hydrological dynamics described during the monitoring period are stationary at decadal timescale. This research demonstrates that speleothems with growth rates <50 μm/yr can also be used for calibration studies. Additionally, we show that the fit of measured and modelled proxy data can be used to achieve annually resolved chronologies in speleothems that were not actively growing at the time of collection and/or that do not record annual laminae.

Key words: Speleothem; Paleoclimate; Calibration; $\delta^{18}O$; Ion microprobe; Postojna

*Corresponding author. Tel: + 385 955256455, E-mail address: ddvillar@hotmail.com (D. Domínguez-Villar).

1. INTRODUCTION

Speleothems can be excellent archives of paleoenvironment and/or paleoclimate (Fairchild and Baker, 2012), and the oxygen isotope composition of speleothems is the most commonly used proxy in speleothem records (e.g., Lauritzen and Lundberg, 1999; Wang et al., 2001; Domínguez-Villar et al., 2017). Most researchers interpret the variability of speleothem $\delta^{18}O$ records in relation to the variability of the inter-annual/long-term oxygen isotope composition of precipitation over the region. However, multiple controls affect the initial $\delta^{18}O$ value of precipitation once the water enters the karst system and before the isotopic composition of drip water is transferred to the speleothems (Lachniet, 2009). Detailed studies have proven that the $\delta^{18}O$ values of speleothems may be dominated by variability of the fractionation factor between the solution and the forming carbonate (Feng et al., 2014). The epikarst hydrology has a significant control on the $\delta^{18}O$ values due to the mixing of groundwater reservoirs with different residence times (Bradley et al., 2010; Baker et al., 2012). Also, the interactive dynamics between the soil and the atmosphere can affect the isotope composition via groundwater evaporation (Ayalon et al., 1998; Markowska et al., 2016) or the thermal decoupling between ground and atmosphere temperature (Domínguez-Villar et al., 2013). Therefore, before conducting detailed paleoenvironmental and/or paleoclimate interpretations from speleothem records, it is desirable to evaluate whether such records can be calibrated with available geochemical, environmental or climatological time series that control the $\delta^{18}O$ values in the system. Previous studies have shown a lack of correlation or a non-stationary relationship between Holocene speleothem $\delta^{18}O$ records and climate variables due to the complexity on the controls affecting the $\delta^{18}O$ values in karst systems (Treble et al., 2005; Fischer and Treble, 2008; Baker et al., 2011). Therefore, it is a good practice to perform calibration tests covering a period lasting no less than a decade in order to conduct robust paleoclimate or paleoenvironmental reconstructions (Burns et al., 2002; Yudava et al., 2004; Jex et al., 2010; Riechelmann et al., 2017).

In order to perform accurate calibration tests, annually resolved chronologies and annual or sub-annual sampling resolutions of the studied proxy are required (e.g., Mattey et al., 2008). Since growth rate is a limiting factor for these studies, speleothems used to calibrate $\delta^{18}O$ records typically have growth rates in the order of several hundred of microns per year. The amount of sample required to perform $\delta^{18}O$ analyses by Gas Source Isotope Ratio Mass Spectrometry (GS-IRMS) limits the spatial sampling resolution along the growth rate of speleothems to a range between 50 and 100 μm in best scenarios (Spötl and Mattey, 2006; Pacton et al., 2013). However, $\delta^{18}O$ analyses can also be carried out using an ion microprobe, which smaller requirements for sample size allows a typical spatial resolution between 10 and 30 μm (Treble et al., 2007; Orland et al., 2009). The use of ion microprobes to study speleothems is not novel, although is still uncommon. This technology has been applied to speleothems to obtain high resolution $\delta^{18}O$ records (Kolodny et al., 2003; Treble et al., 2007), to unravel seasonal cycles (Liu et al., 2015), to study the paleo-seasonality (Orland et al., 2009, 2012, 2015) or to perform calibration of recent samples (Treble et al., 2005; Orland et al., 2014). These studies showed that the spatial resolution of the ion microprobe analyses represents an advantage compared to the combination of micromill sampling and GS-IRMS analyses.

During two years we monitored the water $\delta^{18}O$ values of several drip sites in a hall of Postojna Cave (Slovenia) and selected a laminated speleothem that grew under one of the studied drip sites. Due to the slow growth rate of the top 30 mm of the speleothem (<40 μm/yr), we used ion microprobe analyses to obtain a speleothem $\delta^{18}O$ record of the top 500 μm of the sample that was expected to precipitate over the last decades. The aim of the study is to compare the recent speleothem $\delta^{18}O$ record with the regional record of $\delta^{18}O$ values of precipitation to test whether this speleothem record will provide a robust proxy for the long-term evolution of the $\delta^{18}O$ values of precipitation in the region.

2. MATERIAL AND METHODS

2.1 Postojna Cave and water analyses

Postojna Cave is a 20 km long tourist cave in Slovenia (45.78 ºN; 14.20 ºE). Within this cave, Pisani Rov is a ~0.6 km long corridor aside from the major tourist route. We focus our study on Bela in Rdeča hall (hereafter referred to as BiR hall), which is the last chamber at the far end of Pisani Rov (Fig. 1). BiR hall is 70 m long, 12 m wide and has an average height of 4.5 m. The room is decorated with a multitude of speleothems. This hall has nearly 40 m of bedrock cover (Domínguez-Villar et al., 2015), and there is no appreciable air flow. The surface over the cave has an irregular soil cover dominated by exposed rocks, and according to artificial pits, the soil can locally reach depths >0.5 m. The vegetation consists of a dense mixed forest (i.e., spruce, fir and beech trees). The climate is continental and had a mean annual temperature of 8.7 ºC during the period 1971-2000, with a mean temperature of 18.1 ºC during the warmest month (July) and 0.1 ºC during the coldest month (January). Over the same period, the average amount of annual precipitation was 1590 mm. Snow is common during the winter months and the snow cover over the ground can last for months.

During a 2-year period (2009-2010), we studied the isotope composition of 9 drip sites in BiR hall, all of them located within 40 m (Fig. 1). Drip water samples were collected twice per month for analyses of their oxygen isotope composition. Most of the drip sites had a limited discharge and to accumulate enough water to carry out our analyses, the samples were collected in beakers left under the drip sites since the previous visit. Additionally, a total of 15 beakers containing 50 ml of water with a known initial $\delta^{18}O$ value (+19.16 ‰ VSMOW) were left to equilibrate with the moisture of the cave atmosphere in BiR gallery to evaluate potential evaporation processes. The samples were set under an umbrella to prevent interferences caused by splashing water from nearby drip sites. Water samples of monthly precipitation were also taken at the meteorological station of Postojna. All precipitation, liquid or solid, was collected daily and transferred to a larger bottle that was replaced every month. The bottles were tightly caped to prevent evaporation and kept in a cool and dark place until their transport to the laboratory. The $\delta^{18}O$ values of water samples were determined by equilibration with CO_2 for 12 hours at 25 ºC (Epstein and Mayeda, 1953). The analyses were conducted in an IsoPrime continuous flow GS-IRMS with Multiflow Bio equilibration unit at Jožef Stefan Institute (Slovenia). Measurements were calibrated with two working standards (MiliQ water and snow, calibrated versus VSMOW2 and VSLAP2) and USGS47, USGS48 and USGS49 reference materials were used as controls. Results are reported as ‰ VSMOW and the uncertainty of these measurements is ±0.1 ‰. A stalagmite was collected from one of the studied drip sites (drip site 2). An acoustic drip rate counter

from Driptych (Stalagmate) was installed at this drip site to study the discharge dynamics. The drip rate was recorded at intervals of 10 minutes and integrated into daily drop counts.

2.2 Preparation and analyses of the speleothem

The collected speleothem (PO2) is a 272 mm long stalagmite (Fig. 1). The speleothem was halved along the longitudinal axis and a polished slab was obtained from the central section of the sample. In order to estimate the growth rate of the top of the sample, we calculated U-Th dates from the topmost 30 mm of the stalagmite. We used a hand drill with a 0.9 mm drill bit to obtain 200 to 300 mg of speleothem sample at different distances from the top of the stalagmite following the laminae structure. Sample digestion, spiking and U and Th separation followed a standard procedure (Edwards et al., 1986; Dorale et al., 2004). U and Th isotopes were measured with a NEPTUNE multi collector inductively coupled plasma mass spectrometer at the Department of Geosciences of the University of Minnesota. Ages were calculated according to updated decay constants (Cheng et al., 2013) and assuming an initial $^{230}Th/^{232}Th$ atomic ratio of $4.4 \pm 2.2 \times 10^{6}$. The reported age uncertainty considers 2 standard deviations (SD) of the isotope ratios and its propagation through calculations. Growth rate was calculated using Bayesian statistics by implementing these dates and their uncertainties in the software Oxcal (Ramsey, 2008). We used a P-sequence model of setting "K0" parameter to 0.01 mm^{-1} with a dynamic range from 10^{-2} to 10^{2}.

The central part of PO2 stalagmite has thin visible laminae, keeping a very similar structure throughout the speleothem. We prepared a polished rock section 400 μm thick mounted on a glass plate in order to observe the laminae under optical microscope. From this rock section, we cut a smaller section (3.5 mm wide and 6 mm long) that covers the top of the stalagmite. This small piece of rock section was used to prepare a mount for ion microprobe analyses and to obtain more detailed images of the laminae using a confocal laser fluorescence microscope (CLFM). This mount is an epoxy disc 1-inch in diameter that contains the small portion of the rock section and two grains of UWC-3 (calcite standard; $\delta^{18}O = +12.49$ ‰VSMOW; Kozdon et al., 2009). The section of the speleothem and the standard materials to be analysed by the ion microprobe were arranged within 5 mm of the centre of the mount in order to prevent analytical bias related to the sample position (Valley and Kita, 2005; Kita et al., 2009). The surface of the mount was smoothed and polished using a final polishing solution of colloidal alumina (0.05 μm). Optical microscope and a scanning electron microscope (SEM) were used to check the quality of the polished surface to be sure that sample topography was not larger than 5 μm.

Prior to ion microprobe analyses, the sample mount was cleaned with ethanol and deionised water, dried and subsequently coated with a ~60 nm thick film of gold. In situ analyses of $\delta^{18}O$ were carried out using the WiscSIMS CAMECA ims-1280 large radius multicollector ion microprobe at the University of Wisconsin-Madison. We used a ~1.7 nA primary beam of $^{133}Cs^{+}$ ions, focused to a ~13 μm beam spot at the surface of the sample. The resulting analysis pits were ~1 μm deep and covered a nearly circular ellipse area which minor axis, oriented parallel to the growth axis of the speleothem, was ~13 μm long. Charging of the sample was compensated by an electron flood gun in combination with the gold coating of the mount. Blocks of 4 analyses of the UWC-3 standard were carried out before and after each block of speleothem samples to

calculate the $\delta^{18}O$ value of individual speleothem analysis. Each block of speleothem analyses was limited to a maximum of 15 samples. The reproducibility of individual spot analyses of UWC-3 standard carried out before and after each block of speleothem analyses was assigned as the uncertainty of those speleothem analyses. The average uncertainty of $\delta^{18}O$ analyses during the analytical session was ±0.34 ‰ (2 SD).

Images of fluorescent laminae were obtained after ion microprobe analyses were completed using a Nikon Air Multi-Photon CLFM at the University Image Center of the University of Minnesota, operating with a 488 nm argon-sourced laser line. The images were filtered for wavelengths between 505 and 539 nm. Using these images, laminae were counted in different sectors of the sample to evaluate whether they have an annual periodicity supported by the independent chronological information provided by the U-Th dates.

3. RESULTS

3.1. Cave monitoring

The water $\delta^{18}O$ records of nine cave drip sites monitored during two years show a relatively homogeneous pattern among them (Fig. 2A). The maximum amplitude of the average record is <1 ‰. There is no seasonal pattern in any of the $\delta^{18}O$ records and most of the recorded amplitude results from a 5 month period in the first half of the year 2010 when $\delta^{18}O$ values were on average 0.5 ‰ more negative than during the rest of the record. The water samples left to equilibrate with the moisture of the cave atmosphere showed no sign of volume loss due to evaporation confirming that relative humidity was ~100 % through the year. The $\delta^{18}O$ values of these samples took 3 months to equilibrate with the moisture of the cave atmosphere and afterwards are within 0.2 ‰ of most of the studied drip sites during the same period. Collection of water samples for $\delta^{18}O$ analyses of precipitation on the meteorological station of Postojna started at the onset of the year 2009. The record of $\delta^{18}O$ values of precipitation has a strong seasonality (Fig. 2B) and the annual weighed average $\delta^{18}O$ value of precipitation for the years 2009 and 2010 was -8.4 and -8.3 ‰ VSMOW respectively.

Drip rate that fed the stalagmite PO2 (drip site 2) was studied for over two years. The record shows a complex pattern (Fig. 3), characteristic of drip sites fed by more than one reservoir (Bradley et al., 2010). The drip rate had a characteristic background level of less than 10 drops per day. This pattern was disrupted after certain precipitation events that caused an exponential increase in the drip rate. The sudden change in drip rate after precipitation occurred generally within the same day and rarely exceeded more than 2 days of delay. However, not all precipitation events resulted in a drip rate increase. During autumn and winter, drip rate responded more often to external precipitation events, preventing the drip rate to reach its background level of drip rate. Therefore, autumn and winter months had generally higher drip rates compared to those of spring and summer months.

3.2. Chronology of PO2 top stalagmite

According to the age model, based on five U-Th dates collected between 5 and 28 mm from the top of the speleothem (Table S1 in Supplementary Material), the average growth rate of the top of PO2 stalagmite oscillates between 15 and 40 μm/yr (Fig. 4).

The age model shows that the speleothem grew for more than one millennium since ~1200 yr BP and that it could have been active at the time of collection without any drastic change in growth rate. However, we have not observed precipitation of any calcite on the artificial substrates deployed under drip site 2 during the years of cave monitoring.

The top of PO2 speleothem is a flat surface with a ~50 mm diameter in the centre/axial part of the speleothem. Laminae in the central sector of the speleothem mostly adapt to such flat morphology. The structure of the laminae is very similar along the 272 mm of the speleothem. However, in the top 1.4 mm of the sample we observe three anomalous dark surfaces at 0, 0.5 and 1.4 mm from the top (Fig. 5). Lateral continuity of laminae is occasionally disrupted by these surfaces, especially along small vertical pits (generally <2 mm in depth) showing dissolution of calcite along these surfaces. Therefore, we identify them as hiati, and starting from the top, we name them H1, H2 and H3 (Fig. 4, Fig. 5). The small dissolution features observed at the top of the speleothem suggest that the sample was not growing at the time of collection. These observations are in agreement with the lack of calcite precipitated during the monitoring period in artificial substrates at this site. According to the age model, these three hiati occurred within the last 200 years. Therefore, during this period, variable cave environmental conditions favoured either the PO2 speleothem growth or the formation of hiati. Consequently, despite the chronological uncertainties, the top of PO2 speleothem still has the potential of have been growing during the last decades, when available records of $\delta^{18}O$ values of precipitation can be used for calibration.

PO2 speleothem contains laminae through the sample that could be used to improve the chronology. The thickness of fluorescent laminae range from 2 to 27 μm, and the average thickness is 6 μm (Table S2 in Supplementary Material). The structure and the average thickness of laminae below H3 hiatus do not differ from those above it. The average vertical thickness of speleothem growth per year (growth rate) calculated based on U-Th dates is ~5 times larger than the measured thickness of laminae. Additionally, we identified 81 laminae between H1 and H2 hiati, and 148 laminae between H2 and H3 hiati. According to the age model (assuming a limited change in growth rate, as confirmed by the same average thickness of laminae above and below the hiati) ~175 yr passed since the deposition of the calcite below the H3 hiatus until the time of sample collection. Above H3 hiatus we counted 229 laminae, a number substantially larger than the expected numbers of years until the sample collection. Additionally, this comparison does not consider the duration of the three hiati that would decrease the duration of the available period for the formation of laminae. These evidence confirm that laminae from PO2 stalagmite do not have an annual periodicity and cannot be used to improve the speleothem chronology.

3.3. Speleothem ion microprobe $\delta^{18}O$ analysis

We analysed the $\delta^{18}O$ record of 0.6 mm along the top of PO2 speleothem in situ by ion microprobe. The series of individual analyses were arranged following three parallel lines/transects (A, B and C) oriented perpendicular to the top of the speleothem. Analytical spots are 15 μm apart along the lines to avoid overlapping of the analytical pits. The parallel lines of analyses are only 18 μm apart and analyses of line B are 7.5 μm displaced along the line to provide a dense packing of analyses (Fig. 5). When cracks or other defects on the polished surface occurred along the lines, the location of

the analysis was adjusted laterally, keeping the same distance to the top. The analyses were also conducted below the second hiatus (H2) to test if there is any significant variability across the discontinuity, although the focus of these analyses is to establish a calcite $\delta^{18}O$ record at the top of the stalagmite between hiati H1 and H2.

The results show that the $\delta^{18}O$ variability along the studied lines is within 3 ‰ and the average value is -6.33 ‰ (Fig. 6; Table S3 in Supplementary Material). Before and after the H2 hiatus, the analyses show similar $\delta^{18}O$ values and variability. The records along the three lines nicely replicate each other within analytical uncertainty. Therefore, we integrate the results of the three lines in a composite $\delta^{18}O$ record by averaging the values of the three analytical spots with similar distance to the top of the speleothem (triplets). The ±2 SD envelope of the triplets along the record contains all analyses, and still, the $\delta^{18}O$ variability of the record is larger than this envelope, enabling further study of the isotope variability of the sample. The composite record integrates small lateral and vertical variations of the $\delta^{18}O$ values of calcite, an assumable simplification since the results are still within the analytical uncertainty of the analyses. We used this composite $\delta^{18}O$ record in further calculations of the calibration test.

4. DISCUSSION

4.1. Regional record of $\delta^{18}O$ values of precipitation

PO2 stalagmite was not actively growing at the time of collection and consequently we cannot use the record of $\delta^{18}O$ values of precipitation over Postojna Cave to calibrate our speleothem record. The nearest record of $\delta^{18}O$ values of precipitation is from Ljubljana, located only 40 km northeast of Postojna. The available record of $\delta^{18}O$ values of precipitation from Ljubljana covers the period from 1981 to 2010 (IAEA/WMO, 2009). During the years 2009 and 2010 we have monthly $\delta^{18}O$ values from Postojna and Ljubljana and their $\delta^{18}O$ records have a significant correlation (r^2=0.66; p-value <0.001). The average of the monthly $\delta^{18}O$ values of precipitation is 0.56 ‰ more negative in Ljubljana than in Postojna. The climate in Postojna and Ljubljana, that is expected to control the $\delta^{18}O$ values of precipitation, is very similar. During the years 2009 and 2010 the monthly temperature records of both locations have a strong correlation (r^2=0.99; p-value <0.001), being Postojna in average 1.5 ºC warmer than Ljubljana. The correlation of temperature records and the thermal difference between both sites were stable during the full available instrumental record (Domínguez-Villar et al., 2015). The amount of precipitation recorded in both locations is also correlated (r^2=0.50; p-value <0.001), with Ljubljana having 15% less precipitation than Postojna. However, amount of precipitation is not a significant control of the $\delta^{18}O$ values of precipitation neither in Ljubljana (Vreča et al., 2006) nor in Postojna. Thus, considering an isotope gradient in relation to temperature of 0.30 ‰/ºC, the average difference in the monthly $\delta^{18}O$ values of precipitation between both locations is mostly explained by the cooler temperature recorded in Ljubljana (i.e, based on the temperature control alone, $\delta^{18}O$ values of precipitation in Ljubljana are expected to be on average 0.45 ±0.01 ‰ more negative than in Postojna). Therefore, although other controls could also contribute to the $\delta^{18}O$ values of precipitation in these two sites, it is clear that temperature is a major control of its variability and explains most of the observed differences in the $\delta^{18}O$ values.

The good correlation of $\delta^{18}O$ values of precipitation and its main known control (i.e., temperature) between both locations support the use of Ljubljana $\delta^{18}O$ record as a good indicator of the $\delta^{18}O$ values of precipitation over Postojna cave. Missing data from the Ljubljana $\delta^{18}O$ record (n=23) were calculated assuming temperature as a main control of the $\delta^{18}O$ values of precipitation and considering data within the 95% confidence interval. The resulting equation is: $\delta^{18}O = -12.105 + (0.302 * T)$, where T is the temperature in Ljubljana measured in ºC at 2 m elevation (r^2=0.83, p-value <0.001). The complete record of monthly $\delta^{18}O$ values of precipitation at Ljubljana from 1981 to 2010 and $\delta^{18}O$ weighed annual record are provided in figure 7.

The detailed interpretation of the $\delta^{18}O$ values of precipitation in terms of climate is still under investigation since in addition to temperature, other parameters could explain part of the observed variability. Thus, some authors using weather types have suggested that the source of precipitation could contribute to the $\delta^{18}O$ values of Ljubljana (Brenčič et al., 2015). On the other hand, a preliminary study based on back trajectory analyses and hydro-meteorological models supports that moisture sources have a negligible impact on the $\delta^{18}O$ values over Postojna (Krklec et al., 2016). The discrepancy between these studies confirms the complexity of understanding in depth the climate controls on the $\delta^{18}O$ values of precipitation, a topic beyond the scope of the present study.

4.2. The role of karst hydrology in the transfer of the $\delta^{18}O$ signal

During the two years of monitoring program, the $\delta^{18}O$ signal of the water from studied drip sites showed no seasonality. This is in agreement with a previous study in the same gallery (Vokal, 1999) and implies that the clear seasonality of the $\delta^{18}O$ values of precipitation was filtered out during the transfer of the infiltrated water to BiR hall. However, the drip water $\delta^{18}O$ records are far from being homogeneous during the monitoring period, and the amplitude of the average $\delta^{18}O$ record of all drip is 0.9 ‰. All drip sites showed a similar trend of $\delta^{18}O$ values. Thus, the particular mixing dynamics of percolated water along different routes to each drip site does not modify the $\delta^{18}O$ signal enough to blur the variability provided by the isotope composition of the infiltration water. Therefore, we have developed a model that provides the average $\delta^{18}O$ values of drip sites in BiR hall.

Monthly $\delta^{18}O$ values of precipitation from Postojna were reconstructed back to 1981 using the Ljubljana $\delta^{18}O$ record based on their correlation during the years 2009 and 2010. The model used data from Postojna meteorological station between 1980 and 2010 (i.e., mean monthly temperature, amount of precipitation, snow cover at the end of the month and accumulated amount of snow precipitation). The model considers that all precipitation is infiltrated into the karst, although we account for infiltration delays related to existing snow cover at the end of the moth. During months with snowmelt contribution from a previous month, the monthly $\delta^{18}O$ value of infiltrated water is weighed considering both contributions. The best fit of our model to the averaged record of measured drip water $\delta^{18}O$ values supports a mixing period and transit time in the epikarst of 11 months (r^2=0.72; p-value <0.001) since the moment of infiltration until the water drips in BiR hall (Fig. 8). The correlation of the model is still significant (with p-values <0.001) at 10 and 12 months, although with lower correlation coefficients (r^2=0.56 and 0.50 respectively). The difference between the average $\delta^{18}O$ values of modelled and measured records is within analytical uncertainty, supporting

399 that water evaporation in the system (i.e., soil, epikarst or BiR hall) is negligible or does
400 not affect the drip water $\delta^{18}O$ values.
401
402 Our results show that PO2 speleothem has fluorescent laminae of sub-annual
403 periodicity. Fluorescence in speleothems is related to organic matter derived from the
404 soil that is flushed into the epikarst before being entrapped in the speleothem (e.g.,
405 Baker et al., 1996). A positive relationship has been reported between dissolved organic
406 matter and discharge (Ban et al., 2005). The record of drip rate from drip site 2 shows
407 an exponential increase in discharge associated to precipitation events (Fig. 3). Most of
408 the water discharged by this drip site outflows during these enhanced periods of drip
409 rate, although our isotope monitoring and modelling confirmed that most of infiltrated
410 water requires a delay of 11 months before dripping in BiR hall. Therefore, the quick
411 response of drip rate to precipitation events results from a piston effect (Genty and
412 Deflandre, 1998). Thus, the process of mixing in the karst aquifer filters out any
413 potential seasonal component of dissolved organic matter in the infiltrated water,
414 preventing the fluorescent laminae in PO2 to have seasonal periodicity. Instead, most
415 likely these fluorescent laminae are related to the mixing of at least two reservoirs
416 within the epikarst that have different average concentration of dissolved organic
417 matter. The discharge dynamics recorded in drip site 2 is characteristic of drip sites fed
418 by at least two reservoirs (Bradley et al., 2010). The first reservoir is responsible for the
419 continuous drip rate at a base flow. The second reservoir provides a discontinuous
420 discharge that supplies abundant amount of water only when the piston effect raises its
421 water level causing overflow to the main conduits feeding the drip site. When the
422 second reservoir supplies water to the drip site, the composition of the drip water
423 experiences a mixing proportional to the amount of water supplied by each reservoir,
424 and we observe transitional fluorescence patterns between end members. The reservoir
425 triggering the exponential increase in drip rates does not necessarily involve shorter
426 transit times of the infiltrated water in the aquifer, since its larger volume could
427 compensate the discharge difference with the reservoir providing continuous flow.
428 Thus, the mixing period between most reservoirs in the aquifer may not differ
429 significantly as supported by the homogeneous $\delta^{18}O$ variability recorded in different
430 drip sites in BiR hall.
431
432 According to the average growth rate of PO2 stalagmite provided by the age model, we
433 record in average at least 5 laminae per year. During the monitoring period, the drip rate
434 showed 7 or more events of increased drip rate per year. However, when these events
435 occur too often in a short period of time the drip rate does not decrease to the base flow
436 and number of periods between high and base flow is reduced. During the period when
437 we monitored the drip rate at site 2, the number of events and/or periods with high drip
438 rate recorded was similar to the average number of laminae expected to be recorded
439 every year in the speleothem. Additionally, there is a mechanism that explains the
440 different intensity of fluorescence observed in PO2 laminae, related to the discharge
441 supplied by different reservoirs within the aquifer. Therefore, the hydrological dynamics
442 of drip site 2 supports that the laminae from PO2 stalagmite result from the mixing of at
443 least two reservoirs within the aquifer above BiR hall and that their frequency is related
444 to the events or periods of enhanced discharge which have a sub-annual frequency.
445
446 **4.3. Other controls on the $\delta^{18}O$ record of PO2 stalagmite**
447

Apart from the $\delta^{18}O$ values of drip water, the variability of the speleothem $\delta^{18}O$ record depends on the fractionation factor between the solution and the carbonate and the intra-seasonal growth rate. The water samples left to equilibrate with the moisture of the cave atmosphere did not have any measurable reduction of water volume and their isotope composition does not show signs of evaporation in the cave atmosphere. Therefore, we discard the existence of kinetic fractionation related to evaporation. However, fractionation of oxygen isotopes during the precipitation of calcite depends on temperature (Epstein et al., 1951). At common cave temperatures, these variations have to be larger than 0.4 or 0.5 ºC, depending on the fractionation factor selected (Tremaine et al., 2011 and references therein), to reach the typical uncertainty in $\delta^{18}O$ analyses (i.e., 0.1 ‰). Previous studies in BiR hall showed that inter-annual and intra-annual thermal oscillations are <0.05 ºC (Domínguez-Villar et al., 2015) and consequently, the temperature variability in the cave did not affect the $\delta^{18}O$ record of PO2 speleothem. Since drip water $\delta^{18}O$ values were estimated instead of measured, we only can speculate whether the fractionation of oxygen isotopes between the solution and the calcite at the time of precipitation occurred under equilibrium conditions. However, the average $\delta^{18}O$ value of the top 500 μm of PO2 speleothem is within the range of the predicted isotope composition according to different fractionation factors (e.g., Tremaine et al., 2011) when using the constant temperature of 8.4 ºC in BiR hall during last decades (Domínguez-Villar et al., 2015) and the average $\delta^{18}O$ value of modelled drip water. Therefore, it is reasonable to assume that PO2 speleothem precipitated under near-equilibrium conditions and that the speleothem $\delta^{18}O$ signal records the variability of the $\delta^{18}O$ values of drip water at the time of calcite precipitation.

On the other hand, seasonal growth rate can also determine the $\delta^{18}O$ value of analysed samples from the speleothem. This is not a problem when drip waters have a fairly stable $\delta^{18}O$ signal throughout the year (e.g., Boch et al., 2011). In our case, although the $\delta^{18}O$ values of drip waters do not have a distinctive seasonal component, they record significant variations during the year. This could potentially bias the $\delta^{18}O$ record of a speleothem having seasonal growth rate when compared to the average drip water $\delta^{18}O$ composition. Previous studies on drip sites from the same gallery showed that growth rate lacks seasonality and has a long-term trend resulting from inter-annual variability (Vokal, 1999; Genty et al., 2001). In the case of the PO2 speleothem, its growth rate could be enhanced during periods of increased discharge. Events of increased drip rate occurred more often at drip site 2 during the autumn and winter months, when enhanced advection in BiR hall facilitated higher discharge rates after certain precipitation events (Domínguez-Villar et al., 2015). However, during spring and summer the cumulative duration of periods with drip rate above the base flow was not necessarily shorter than their cumulative duration in autumn and winter (Fig. 3). In any case, we do not discard that potential intra-annual growth rate variability of the PO2 speleothem could have introduced certain noise to the average speleothem $\delta^{18}O$ record when compared to the average drip water $\delta^{18}O$ values during the same period. However, we do not expect a systematic bias of the recorded speleothem $\delta^{18}O$ values due to the absence of a seasonal drip water $\delta^{18}O$ oscillation. The limited impact of the intra-seasonal variability of growth rate on the $\delta^{18}O$ values of the speleothem is supported by the coincidence within the uncertainties of the average composition of PO2 $\delta^{18}O$ record and the expected value of precipitated calcite from all the modelled drip water $\delta^{18}O$ values under equilibrium conditions.

4.4. Calibration of the $\delta^{18}O$ record of PO2 stalagmite

We cannot establish an accurate chronology for the top 500 μm of PO2 stalagmite based on radiometric methods or counting laminae. However, according to the age model based on U-Th dates, PO2 speleothem grew continuously, with a narrow average growth rate range (i.e., 15 to 40 μm/yr), during a millennium until ~175 yr ago. Since that moment, 5 episodes were recorded by the speleothem in its uppermost 1400 μm: 3 hiati and 2 periods of speleothem growth. Since there is no difference in the average thickness of laminae above or below the hiati (Table S2 in Supplementary Material), the average growth rate is expected to be similar for the periods of calcite precipitation above and below the hiati. Thus, considering the above mentioned range of growth rate, the section of the speleothem between H3 and H2 hiati (i.e., 1400 to 500 μm from the top) could record 23 to 60 years of speleothem growth, while the section of the speleothem between H2 and H1 (i.e., topmost 500 μm) could record 13 to 34 yr of speleothem growth. Although the duration of the hiati is unknown, it is plausible that the topmost 500 μm of the speleothem could have been precipitated during the last decades.

The variability of the annual weighed $\delta^{18}O$ values of Ljubljana precipitation and the $\delta^{18}O$ record of the top of PO2 speleothem shows outstanding similarities (Fig. 6 and Fig. 7). Therefore, based on the available chronological evidence and the assumption that the variability of $\delta^{18}O$ of drip waters will be mostly captured by the speleothem, we assigned a tentative chronology to the top 500 μm of PO2 stalagmite. We do it by optimising the correlation coefficient between the modelled drip water $\delta^{18}O$ signal and the $\delta^{18}O$ record from PO2 speleothem.

The data of modelled drip water $\delta^{18}O$ values considered a reference time period of 11 months, which is the mixing and transit time determined by our model in agreement with the monitoring data. The speleothem $\delta^{18}O$ values were integrated into portions of the speleothem that could have precipitated during periods of ~11 months. The best fit of data required integrating 1 to 3 analyses per period of 11 months and a single analysis was not assigned to more than one period. This integration of portions of the speleothem along the vertical axis of the sample could represent growth rates for individual periods of 11 months ranging from 14 to 50 μm, which is in good agreement with the average growth rate previously reported. The best fit between the speleothem $\delta^{18}O$ record and the modelled drip water $\delta^{18}O$ signal (Fig. 9) suggests that the topmost 500 μm of the speleothem precipitated during 18 years (i.e., 21 periods of 11 months) between the years 1984 and 2002 (r^2=0.84; p-value<0.001). According to this tentative age model, the average growth rate of this portion of the speleothem was 27 μm/yr, which is exactly the same average growth rate that we calculated below the H3 hiatus.

The tentative age model produces a good correlation between the $\delta^{18}O$ records of the modelled drip water and the speleothem. However, is this correlation the result of two synchronous records with a causal relationship, or could be a casual correlation of two independent time series? Large correlation factors are artificially enhanced by limited number of data that do not capture most of the variability of the studied parameters or by the existence of unrelated long-term trends in both series. We have a series with 21 data, and in our case a minimum of 7 data are required to reproduce results within a 95% confidence. On the other hand, none of these records have any particular long-term

trend, but instead they have characteristic oscillations of variable amplitude. Correlated time series with such a complex signal structure are likely to have a common forcing. In any case, we explore the possibility that the modelled drip water $\delta^{18}O$ record could have such a good correlation (r^2=0.84) with a random time series. We have developed one million virtual speleothem $\delta^{18}O$ records and compared them to the modelled drip water $\delta^{18}O$ signal between the years 1984 and 2002. The virtual speleothem records were produced randomly within the variability (i.e., 2 SD) of the $\delta^{18}O$ values of the modelled drip water between 1984 and 2002. The maximum correlation obtained in all simulations (i.e., r^2= 0.71; p-value<0.001) was well below the reported correlation coefficient. In the last 175 years there are ~190 periods of 11 months and less than 170 combinatory options to distribute a continuous record of 18 years. This analysis shows that considering the combinatory constraints, the possibility to obtain such a good correlation between both records randomly is negligible. Therefore, we can confirm the tentative age model for the topmost 500 μm of PO2 speleothem. This calibration test shows that the $\delta^{18}O$ record of PO2 speleothem accurately records the isotope composition of precipitation over the region filtered through the epikarst.

5. CONCLUSIONS

We used an ion microprobe to analyse the $\delta^{18}O$ record of a slow growth rate speleothem precipitated until recent times in Postojna Cave. The speleothem was not actively forming at the time of collection, although U-Th dates support its growth until recent times. Fluorescent laminae in the speleothem had sub-annual frequency and could not be used to establish an annually resolved chronology. On the other hand, we modelled the $\delta^{18}O$ composition of drip water in the studied cave, using a regional $\delta^{18}O$ record of precipitation with monthly resolution. The model was validated using water $\delta^{18}O$ composition of several drip sites measured during a 2-year monitor period. The results suggest that water had a transit and mixing time of 11 months after its infiltration in the aquifer. The comparison of the speleothem $\delta^{18}O$ record with the modelled $\delta^{18}O$ composition of drip water confirmed that the speleothem precipitated during the years 1984 and 2002. The annually resolved age model during this period was based on the best correlation of these two records supported by the additional chronological information available. We also conclude that the $\delta^{18}O$ signal of the speleothem records the inter-annual variability of the regional $\delta^{18}O$ composition of precipitation without any seasonal bias, and that the hydrological dynamics recorded during the monitoring period are stationary at decadal timescale.

This research shows the potential of ion microprobe analyses to perform calibration tests on recent speleothems with slow growth rates. Additionally, we demonstrated that calibration tests at annual resolution are still possible in samples not actively growing at the time of collection. We have also shown that under certain circumstances it is possible to achieve annually resolved speleothem chronologies from speleothems lacking annual laminae.

ACKNOWLEDGEMENTS

We thank Postojnska jama d.d. and the Ministry of Environment and Spatial Planning of Slovenia for the permissions to access the cave and to sample the speleothem. We appreciate the support of Stanislav Glažar, who joined us in every visit to the cave

during the monitoring period. We are grateful to Andrej Mihevc from the Karst Research Institute in Postojna who supervised the speleothem collection in the cave. Ion probe analyses were conducted in WiscSIMS laboratory at the University of Wisconsin-Madison thanks to the essential support and advice of John W. Valley. We thank Ian J. Orland and Kathleen A. Wendt for their discussion and support in the analytical design and the fluorescence imaging of PO2 stalagmite. We thank Stojan Žigon for water stable isotope analyses at Jožef Stefan. One of the authors (SL) received funds from the ARRS research programme P1-0143 and the EU Horizon 2020 project MASSTWIN (grant agreement No. 692241).

REFERENCES

Ayalon, A., Bar-Matthews, M. and Sass, E. (1998) Rainfall-recharge relationships within a karstic terrain in the Eastern Mediterranean semi-arid region, Israel: $\delta^{18}O$ and δD characteristics. *Journal of Hydrology* **207**, 18-31.

Baker, A., Barnes, W.L. and Smart, P.L. (1996) Speleothem luminescence intensity and spectral characteristics: signal calibration and record of palaeovegetation. *Chemical Geology* **130**, 65-76.

Baker, A., Wilson, R., Fairchild, I.J., Franke, J., Spötl, C., Mattey, D., Trouet, V. and Fuller, L. (2011) High resolution $\delta^{18}O$ and $\delta^{13}C$ records from an annually laminated Scottish stalagmite and relationship with last millennium climate. *Global and Planetary Change* **79**, 303-311.

Baker, A., Bradley, C., Phipps, S.J., Fischer, M., Fairchild, I.J., Fuller, L., Spötl, C. and Azcurra, C. (2012) Millennial-length forward models and pseudoproxies of stalagmite $\delta^{18}O$: an example from NW Scotland. *Climate of the Past* **8**, 1153-1167.

Ban, F., Pan, G. and Wang. X. (2005) Timing and possible mechanism of organic substance formation in stalagmite laminae from Beijing Shihua Cave. *Quaternary Sciences* **25**, 265-268. (in Chinese).

Boch, R., Spötl, C. and Frisia, S. (2011) Origin and palaeoenvironmental significance of lamination in stalagmites from Katerloch Cave, Austria. *Sedimentology* **58**, 508-531.

Bradley, C., Baker, A., Jex, C.N. and Leng, M.J. (2010) Hydrological uncertainties in the modelling of cave drip-water $\delta^{18}O$ and the implications for stalagmite palaeoclimate reconstructions. *Quaternary Science Reviews* **29**, 2201-2214.

Brenčič, M., Kononova, N.K. and Vreča, P. (2015) Relation between isotopic composition of precipitation and atmospheric circulation patterns. *Journal of Hydrology* **529**, 1422-1432.

Burns, S.J., Fleitmann, D., Mudelsee, M., Neff, U., Matter, A. and Mangini, A. (2002) A 780-year annually resolved record of Indian Ocean monsoon precipitation from a speleothem from south Oman. *Journal of Geophysical Research* **107(D20)**, 4434.

Cheng, H., Edwards, R.L., Shen, C.C., Polyak, V.J., Asmerom, Y., Woodhead, J., Hellstrom, J., Wang, Y., Kong, X., Spötl, C., Wang, X. and Alexander, E.C. (2013) Improvements in ^{230}Th dating, ^{230}Th and ^{234}U half-life values, and U-Th isotopic measurements by multi-collector inductively coupled plasma mass spectrometry. *Earth and Planetary Science Letters* **371-372**, 82-91.

Domínguez-Villar, D., Fairchild, I.J., Baker, A., Carrasco, R.M. and Pedraza, J. (2013) Reconstruction of cave air temperature based on surface atmosphere temperature and vegetation changes: implications for speleothem paleoclimate records. *Earth and Planetary Science Letters* **369-370**, 158-168.

643 Domínguez-Villar, D., Lojen, S., Krklec, K., Baker, A. and Fairchild, I.J. (2015) Is
644 global warming affecting cave temperature? Experimental and model data from a
645 paradigmatic case study. *Climate Dynamics* **45**, 569-581.
646 Domínguez-Villar, D., Wang, X., Krklec, K., Cheng, H. and Edwards, R.L. (2017) The
647 control of the tropical North Atlantic on Holocene millennial climate oscillations.
648 *Geology* **45**, 303-306.
649 Dorale, J.A., Edwards, R.L., Alexander, E.C.Jr., Shen, C.C. and Richards, D.A. (2004)
650 Uranium series dating of speleothems: Current techniques, limits & applications. In
651 *Studies of Cave Sediments* (eds. I.D. Sasowsky and J.E. Mylroie), Kluwer
652 Academic/Plenum Publishers, New York, pp. 177-198.
653 Edwards, R.L., Chen, J.H. and Wasserburg, G.J. (1986) 238U-234U-230Th-232Th
654 systematics and the precise measurements of time over the past 500,000 years. *Earth*
655 *and Planetary Science Letters* **81**, 175-192.
656 Epstein, S., Buchsbaum, R., Lowenstam, H. and Urey, H. C. (1951) Carbonate-water
657 isotopic temperature scale. *Geological Society of America Bulletin* **62**, 417-426.
658 Epstein, S. and Mayeda, T. (1953) Variation of O^{18} content of waters from natural
659 sources. *Geochimica et Cosmochimica Acta* **4**, 213-224.
660 Fairchild, I.J. and Baker, A. (2012) Speleothem science: from processes to past
661 environments. Wiley-Blackwell, Chichester.
662 Feng, W., Casteel, R.C., Banner, J. and Heinze-Fry, A. (2014) Oxygen isotope
663 variations in rainfall, drip water and speleothem calcite from a well-ventilated cave in
664 Texas, USA: Assessing a new speleothem temperature proxy. *Geochimica et*
665 *Cosmochimica Acta* **127**, 233-250.
666 Fischer, M.J. and Treble, P.C. (2008) Calibrating climate-$\delta^{18}O$ regression models for
667 the interpretation of high-resolution speleothem $\delta^{18}O$ time series. *Journal of*
668 *Geophysical Research* **113**, D17103.
669 Genty, D. and Deflandre, G. (1998) Drip flow variations under a stalactite of the Père
670 Noel cave (Belgium). *Journal of Hydrology* **211**, 208-232.
671 Genty, D., Baker, A. and Vokal, B. (2001) Intra- and inter-annual growth rate of
672 modern stalagmites. *Chemical Geology* **176**, 191-212.
673 IAEA/WMO, 2009. Global network of isotopes in precipitation. The GNIP database.
674 Accessible at: http://www.iaea.org/water.
675 Jex, C.N., Baker, A., Leng, M.J., Sloane, H.J., Eastwood, W.J., Fairchild, I.J., Thomas,
676 L. and Bekaroglu, E. (2010) Calibration of speleothem $\delta^{18}O$ with instrumental climate
677 records from Turkey. *Global and Planetary Change* **71**, 207-217.
678 Kita, N.T., Ushikubo, T., Fu, B. and Valley, J.W. (2009) High precision SIMS oxygen
679 isotope analices and the effect of simple topography. *Chemical Geology* **264**, 43-57.
680 Kolodny, Y., Bar-Matthews, M., Ayalon, A. and McKeegan, K.D. (2003) A high spatial
681 resolution $\delta^{18}O$ profile of a speleothem using an ion-microprobe. *Chemical Geology*
682 **197**, 21-28.
683 Kozdon, R., Ushikubo, T., Kita, N.T., Spicuzza, M. and Valley, J.W. (2009) Intratest
684 oxygen isotope variability in the planktonic foraminifer *N. pachyderma*: real vs.
685 apparent vital effects by ion microprobe. *Chemical Geology* **258**, 327-337.
686 Krklec, K., Domínguez-Villar, D. and Lojen, S. (2016) Moisture sources of
687 precipitation over Postojna (Slovenia) and implication of its isotope composition.
688 *Geophysical Research Abstracts* **18**, EGU2016-3910.
689 Lachniet, M.S. (2009) Climatic and environmental controls on speleothem oxygen-
690 isotope values. *Quaternary Science Reviews* **28**, 412-432.

691 Lauritzen. S.E., Lunberg, J. (1999) Calibration of the speleothem delta function: an
692 absolute temperature record for the Holocene in northern Norway. *The Holo*cene **9**,
693 659-669.
694 Liu, Y.H., Tang, G.Q., Ling, X.X., Hu, C.Y. and Li, X.H. (2015) Speleothem annual
695 layers revealed by seasonal SIMS $\delta^{18}O$ measurements. *Science China Earth Science*
696 **58**, 1741-1747.
697 Markowska, M., Baker, A., Andersen, M.S., Jex, C.N., Cuthbert, M.O., Rau, G.C.,
698 Graham, P.W., Rutlidge, H., Mariethoz, G., Marjo, C.E., Treble, P.C. and Edwards,
699 N. (2016) Semi-arid zone caves: evaporation and hydrological controls on $\delta^{18}O$ drip
700 water composition and implications for speleothem paleoclimate reconstructions.
701 *Quaternary Science Reviews* **131**, 285-301.
702 Mattey. D., Lowry, D., Duffet, J. Fisher, R., Hodge, E., and Frisia, S. (2008) A 53 year
703 seasonally resolved oxygen and carbon isotope record from a modern Gibraltar
704 speleothem: Reconstructed drip water and relationship to local precipitation. *Earth*
705 *and Planetary Science Letters* **269**, 80-95.
706 Orland, I.J., Bar-Matthews, M., Kita, N.T., Ayalon, A., Matthews, A. and Valley, J.W.
707 (2009) Climate deterioration in the Eastern Mediterranean as revealed by ion
708 microprobe analyses of a speleothem that grew from 2.2 to 0.9 ka in Soreq Cave,
709 Israel. *Quaternary Research* **71**,27-35.
710 Orland, I.J., Bar-Matthews, M., Ayalon, A., Matthews, A., Kozdon, R., Ushikubu, T.
711 and Valley, J.W. (2012) Seasonal resolution of Eastern Mediterranean climate change
712 since 34 ka from Soreq Cave speleothem. *Geochimica et Cosmochimica Acta* **89**, 240-
713 255.
714 Orland I.J., Burstyn, Y., Bar-Matthews, M., Kozdon, R., Ayalon, A., Matthews, A. and
715 Valley, J.W. (2014) Seasonal climate signals (1990-2008) in a modern Soreq Cave
716 stalagmite as revealed by high-resolution geochemical analyses. *Chemical Geology*
717 **363**, 322-333.
718 Orland, I.J., Edwards, R.L., Cheng, H., Kozdon, R., Cross, M. and Valley, J.W. (2015)
719 Direct measurements of deglacial monsoon strength in a Chinese stalagmite. *Geology*
720 **43**, 555-558.
721 Pacton, M., Breitenbach, S.F.M., Lechleitner, F.A., Vaks, A., Rollion-Bard, C.,
722 Gutareva, O.S., Osintcev, A.V. and Vasconcellos, C. (2013) The role of
723 microorganisms in the formation of a stalactite in Botovskaya Cave, Siberia -
724 Paleoenvironmental implications. *Biogeosciences* **10**, 6115-6130.
725 Ramsey, C.B. (2008) Deposition models for chronological records. *Quaternary Science*
726 *Reviews* **27**, 42-60.
727 Riechelmann, S., Schröder-Ritzrau, A., Spötl, C., Riechelmann, D.F..C., Richter, D.K.,
728 Mangini, A., Frank, R., Breitenbach, S.F.M. and Immenhauser, A. (2017) Sensitivity
729 of Bunker Cave to climatic forcings highlighted through multi-annual monitoring of
730 rain-, soil-, and dripwaters. *Chemical Geology* **449**, 194-205.
731 Spötl, C. and Mattey, D. (2006). Stable isotope microsampling of speleothems for
732 palaeoenvironmental studies: A comparison of microdrill, micromill and laser ablation
733 techniques. *Chemical Geology* **235**, 48-58.
734 Treble, P.C., Chappell, J., Gagan, M.K., McKeegan, K.D. and Harrison, T.M. (2005) In
735 situ measurements of seasonal $\delta^{18}O$ variations and analysis of isotopic trends in a
736 modern speleothem from southwest Australia. *Earth and Planetary Science Letters*
737 **233**, 17-32.
738 Treble, P.C., Schmidt, A.K., Edwards R.L., McKeegan, K.D., Harrison, T.M., Grove
739 M., Cheng, H. and Wang, Y.J. (2007) High resolution Secondary Ionization Mass

740 Spectrometry (SIMS) $\delta^{18}O$ analyses of Hulu Cave speleothem at the time of Heinrich
741 Event 1. *Chemical Geology* **238**, 197-212.
742 Tremaine, D.M., Froelich, P.N. and Wang, Y. (2011) Speleothem calcite farmed in situ:
743 Modern calibration of $\delta^{18}O$ and $\delta^{13}C$ paleoclimate proxies in a continuously-
744 monitored natural cave system. *Geochimica et Cosmochimica Acta* **75**, 4929-4950.
745 Valley, J.W. and Kita, N.T. (2005) First results from UW CAMECA IMS-1280. Fourth
746 Biennial Geochemincal SIMS workshop.
747 Vokal, B. (1999) The carbon transfer in karst areas – An application to the study of
748 environmental changes and paleoclimatic reconstruction. Ph. D. Thesis. School of
749 Environmental Sciences, Polytechnic Nova Gorica (Slovenia).
750 Vreča, P., Krajcar Bronić, I., Horvatinčić, N. and Barešić, J. (2006) Isotopic
751 characteristics of precipitation in Slovenia and Croatia: comparison of continental and
752 marine stations. *Journal of Hydrology* **330**, 457-469.
753 Wang, Y., Cheng, H., Edwards, R.L., An, Z., Wu, J., Shen, C.C. and Dorale, J.A. (2001)
754 Absolute-dated Late Pleistocene monsoon record from Hulu Cave, China. *Science*
755 **294**, 2345-2348.
756 Yudava, M.G., Ramesh, R. and Pant, G.B. (2004) Past monsoon rainfall variations in
757 peninsular India recorded in a 331-year old speleothem. *The Holocene* **14**, 517-524.
758

FIGURES

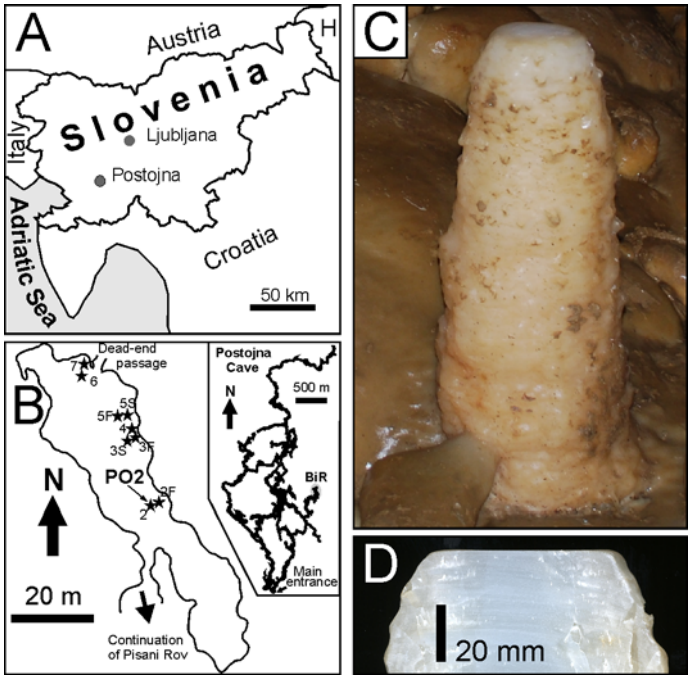

Figure 1. Location map, cave sketch and speleothem images. A: Location map of Slovenia. Records of $\delta^{18}O$ values of precipitation are from Ljubljana and Postojna. The studied cave is in Postojna. B: Sketch of BiR hall (plan view) showing the location of drip sites (stars). Studied speleothem (PO2) was collected from drip site 2. The inlet graph shows the location of BiR hall within Postojna Cave (grey shaded area). C: Image of stalagmite PO2 before collection. The sample is 272 mm long. D: Detailed image of the top 30 mm of PO2 speleothem showing the flat surface of the centre of the speleothem.

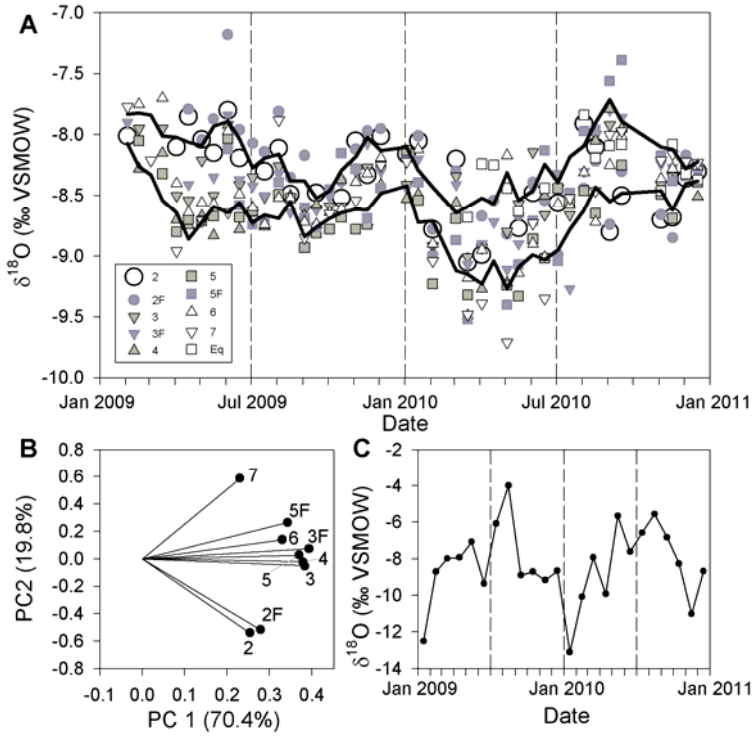

Figure 2. Records of $\delta^{18}O$ values of BiR drip water and Postojna precipitation during the years 2009 and 2010. A: Water $\delta^{18}O$ values of 9 drip sites of BiR hall. Black bold lines represent the upper and lower boundary of the 1 standard deviation of the 9 drip site records for every observational period, plotted from their average $\delta^{18}O$ value. The record of water equilibrated with the moisture of the cave atmosphere (eq) is also shown. B: Monthly record of Postojna $\delta^{18}O$ values of precipitation.

780

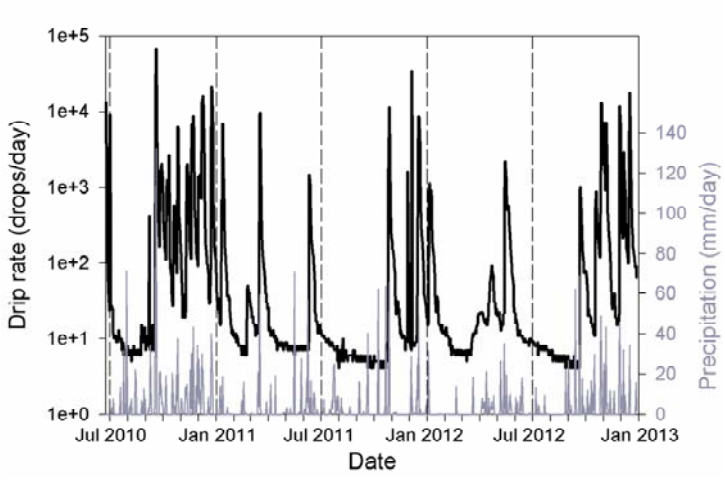

781
782

783 Figure 3. Records of drip rate at site 2 and amount of precipitation measured in Postojna
784 meteorological station.

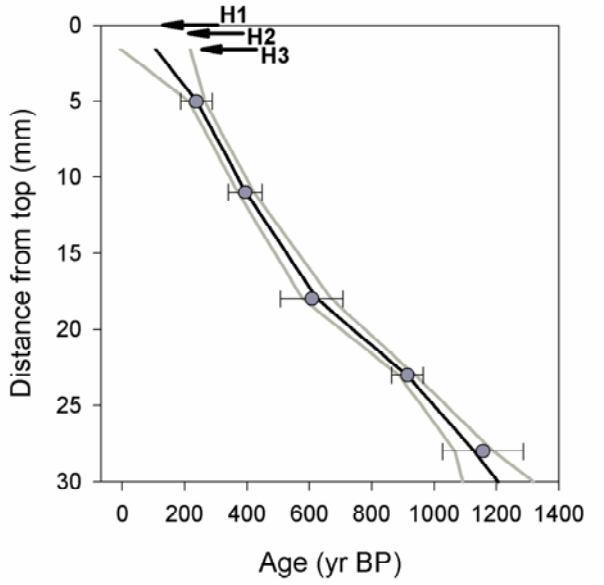

Figure 4. Age model of PO2 speleothem between 1.4 and 30 mm from the top of the sample (black line). Grey lines represent the uncertainty of the age model. H1, H2 and H3 are three hiati identified at 0, 0.5 and 1.4 mm from the top of the sample. Grey dots and error bars are the U-Th dates and their uncertainties.

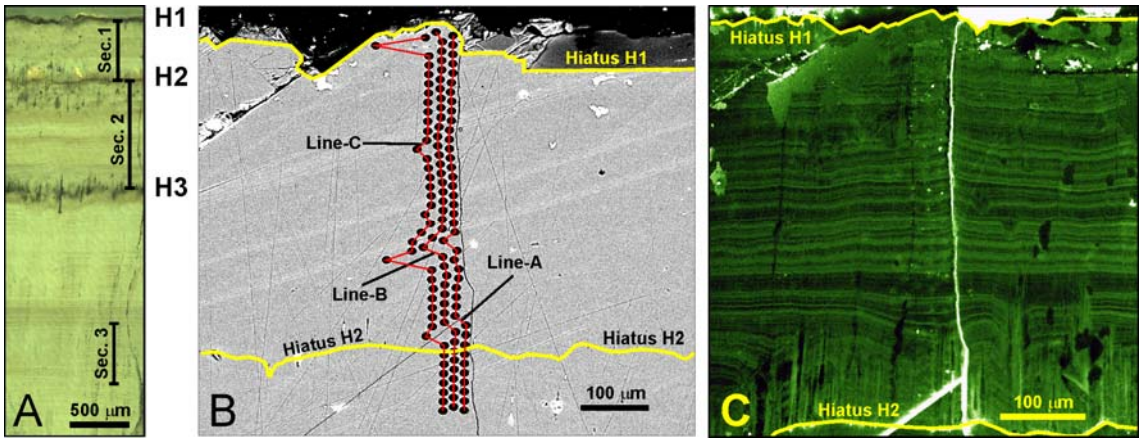

Figure 5. Microscope imaging of PO2 speleothem. A: Optical microscope image of top 3.5 mm of PO2 speleothem. Three hiati (H1, H2 and H3) are clearly visible. Vertical capped lines identify the three sections were laminae were counted (see Table S2 in Supplementary Material). B: Scanning electron microscope image showing the ion microprobe sampling routine along 3 different lines. Black ellipses show the dimension of every analytical spot. Yellow lines are hiati surfaces. Hiatus H1 is at the top of the speleothem regardless the false impression of the image due to different focal planes. C: Confocal laser fluorescence microscope image of the top 500 µm of PO2 speleothem showing fluorescent laminae. The thickness of fluorescent laminae is thinner than the size of the analytical spots of the ion microprobe analyses, preventing the study of intra-laminae $\delta^{18}O$ variability. White lines are cracks, whereas black areas represent material without fluorescence. The patchy sections with fluorescence patterns disrupting the laminae are the result of areas where the gold coat was not properly removed before imaging.

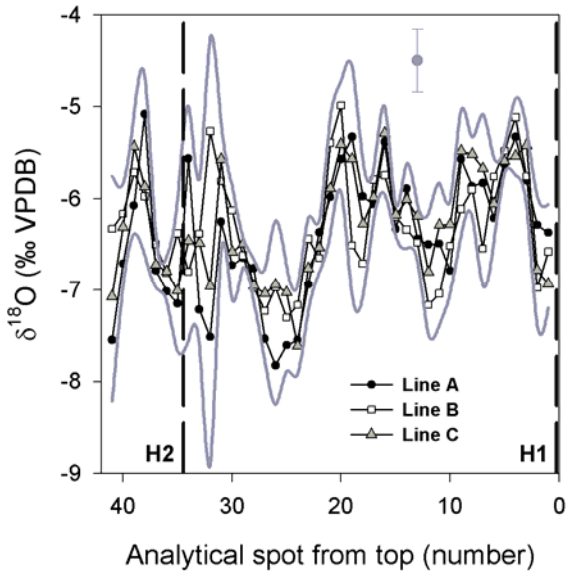

Figure 6. Ion microprobe $\delta^{18}O$ analyses of the top 600 μm of PO2 speleothem along three parallel lines. The location of hiati H1 and H2 are represented by the black vertical dashed lines. The dot with error bars represents the average uncertainty of ion microprobe analyses. Grey lines are the upper and lower boundaries of the 2 standard deviations of the 3 samples at similar distance from the top of the speleothem along the 3 parallel sampling lines, plotted from their average $\delta^{18}O$ value.

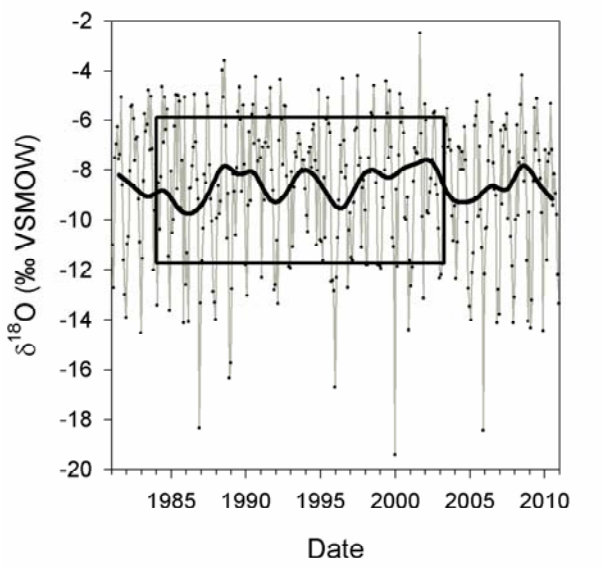

Figure 7. Record of monthly $\delta^{18}O$ values of precipitation from Ljubljana. The record of annual weighed isotope values is represented as a black bold line. The rectangle highlights the period between the years 1984 and 2002 (both included).

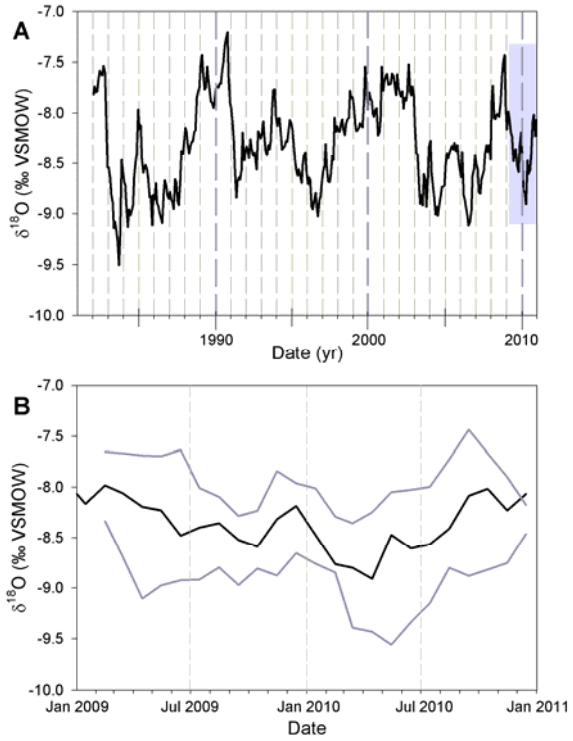

Figure 8. Model of monthly $\delta^{18}O$ values of drip water in BiR hall using an infiltration mixing and transit time period of 11 months. A: Record of the modelled $\delta^{18}O$ values of drip water during the period 1982-2011. The grey box during the years 2009 and 2010 represent the period expanded in panel B. B: Comparison of $\delta^{18}O$ records of drip waters from the model and the monitoring period. The black line represents the record of the modelled $\delta^{18}O$ values of drip water during the years 2009 and 2010. The grey lines represent the upper and lower limits of the 2 standard deviations of the monthly $\delta^{18}O$ values observed in the 9 drip sites, plotted from their average $\delta^{18}O$ values.

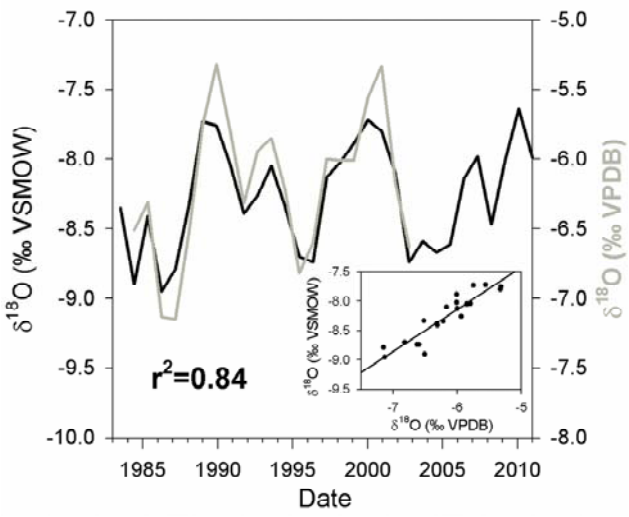

Figure 9. Comparison of the record of modelled drip water $\delta^{18}O$ values in BiR hall weighed for 11 months periods from the year 1983 until 2011 and the record of $\delta^{18}O$ values of PO2 speleothem using a tentative age model that optimises the correlation of the data. See text for further details.